JOURNAL OF VIROLOGY, July 1984, p. 199–207
0022-538X/84/070199-09$02.00/0

Vol. 51, No. 1

Structure of Defective DNA Molecules in Epstein-Barr Virus Preparations from P3HR-1 Cells

MYUNG-SAM CHO,†* GEORG W. BORNKAMM, AND HARALD ZUR HAUSEN‡

Institut für Virologie, Zentrum für Hygiene, Universität Freiburg, 7800 Freiburg, Federal Republic of Germany

Received 16 November 1983/Accepted 16 March 1984

Epstein-Barr virus (EBV), isolated from P3HR-1 cells, induces early antigen and viral capsid antigen upon infection of human B-lymphoblasts. The strong early antigen- and viral capsid antigen-inducing activity is only observed in P3HR-1 virus preparations harboring particles with defective genomes, suggesting that this biological activity is directly associated with the defective DNA population. After infection of EBV genome-carrying Raji or EBV genome-negative BJAB cells, defective genomes of P3HR-1 EBV DNA are replicated in excess, depending on the multiplicity of infecting EBV particles. Hybridization of the DNA from such infected cells with ^{32}P-labeled EBV DNA after *Hin*dIII cleavage reveals six hypermolar fragments. Mapping of these fragments shows that they form one defective genome unit containing four nonadjacent regions (α, β, γ, and δ) of the nondefective P3HR-1 EBV DNA. Two of the segments (α and β) contain ca. 17 and 13 megadaltons, respectively, from the terminal regions of the P3HR-1 genome, whereas the two smaller segments (γ and δ) contain ca. 3.7 and 3.0 megadaltons, respectively, originating from the central portion of the genome. In the defective molecule, the regions γ and δ are present in the opposite orientation compared with nondefective P3HR-1 EBV DNA. Tandem concatemers are formed by fusion of the α and β regions. Our model suggests that tandem concatemers of three defective genome units can be packaged into virions in P3HR-1 cells.

Epstein-Barr virus (EBV) derived from the P3HR-1 subclone of the Burkitt lymphoma line Jijoye (13) reveals some biological properties distinct from other EBV isolates characterized thus far. The virus does not transform human B-lymphocytes (19), although infection of cells with this virus leads to induction of the EBV-specific nuclear antigen EBNA (18). Two distinct patterns of EBNA have been revealed in P3HR-1 EBV-infected B-lymphocytes (9, 18), and cloned sublines expressing one of these types have been obtained (8). In contrast to other EBV isolates, P3HR-1 EBV efficiently induces early antigens upon infection of various lymphoblastoid lines of B-cell origin (11). Although this infection is largely abortive, a few cells have been shown to enter the late stage of virus replication, and virus particle synthesis has been demonstrated (4, 7, 17, 27, 28).

The DNA of P3HR-1 EBV has been characterized by partial denaturation mapping (5) and by restriction enzyme analysis (1, 10). These studies revealed a remarkable heterogeneity of P3HR-1 virus DNA. The heterogeneity is even more pronounced after analysis of EBV DNA from P3HR-1 EBV-infected lymphoblasts (4, 17, 24). The fragment pattern of EBV DNA in those cells obtained after cleavage with the restriction endonuclease *Hin*dIII consistently shows six hypermolar fragments in addition to the viral fragments observed in molar ratios. This pattern is independent of the target cells used for infection and does not depend on the presence or absence of EBV DNA in these cells before infection with P3HR-1 EBV (4). The hypermolar fragments appear to be derived from defective DNA molecules (4). Most interestingly, by subcloning of P3HR-1 cells it could be demonstrated that high spontaneous virus production and high early antigen-inducing activity of virus preparations are both dependent on the presence of defective genomes (22). This strongly suggests that the defective genomes exert direct biological functions associated with the induction of the lytic cycle.

Relatively little is known about the structural organization of the defective genomes. The most detailed study was reported by Heller et al. (10), who showed by using cloned EBV DNA probes that the defective molecules consist of distinct pieces of EBV DNA which are not adjacent in the genomes of nondefective virus particles. How these pieces are precisely arranged to each other in the defective genomes, however, has not been unraveled. Therefore, in an attempt to study the biological functions of the defective genomes, we first had to elucidate their structural organization.

In P3HR-1 virus-infected BJAB cells, the analysis of the defective genomes is facilitated by the fact that these cells do not contain endogenous viral genomes. After infection with the virus, the defective genomes are preferentially replicated and represent the vast majority of viral sequences in these cells. Here we report studies on the detailed structure of the defective genomes isolated after infection of EBV-negative BJAB cells with high particle multiplicities of P3HR-1 EBV.

MATERIALS AND METHODS

Cell lines. The virus-producing cell line P3HR-1 (13), the EBV nonproducer line Raji (20), and the EBV genome-negative line BJAB (15) are routinely kept in our laboratory. Cell line P3HR-1, HR-1 clone II that was used for infection was kindly supplied by W. Henle, Philadelphia, Pa. All cells were grown in RPMI 1640 medium supplemented with 10% fetal calf serum and antibiotics and were fed once or twice weekly.

Virus sedimentation. Virus-producing cell cultures were grown to a density of 10^6 cells per ml at 37°C and fed once a week. To increase the virus yield, the tumor promoter 12-*O*-

* Corresponding author.
† Present address: Department of Pharmacology and Experimental Therapeutics, The Johns Hopkins University School of Medicine, Baltimore, MD 21205.
‡ Present address: Deutsches Krebsforschungszentrum, im Neuenheimer Feld 280, 6900 Heidelberg, Federal Republic of Germany.

tetradecanoylphorbol-13-acetate was added to a final concentration of 20 ng/ml (29, 30). For radioactive labeling of virus, cells were kept in medium containing 1 μl of [^{3}H]thymidine per ml (specific activity, 21 Ci/mol; Radiochemical Centre, Amersham, Buckinghamshire, England). Virus was sedimented from supernatants of aged cells at 9,000 rpm for 150 min (rotor GSA; Ivan Sorvall, Inc., Norwalk, Conn.) as described previously (4). For infection experiments, sedimented virus was resuspended at a 2,000-fold concentration in medium and filtered (pore size, 0.45 μm; Millipore Corp., Bedford, Mass.) before use.

Infection with P3HR-1 EBV. BJAB cells were infected after completion of the procedure described previously (4). Briefly, 20×10^6 cells, subcultured 2 days before infection, were sedimented and infected with 2 ml of the 12-*O*-tetradecanoylphorbol-13-acetate-activated virus concentrate by incubating them for 90 min at 37°C in humidified 5% CO_2. After adsorption, the cells were washed five times with medium and then resuspended in 20 ml of fresh RPMI 1640 medium supplemented with 20% fetal calf serum. After incubation for 4 days the cells were sedimented, and the DNA was extracted by phenol.

Preparation of viral DNA. Sedimented pellets of concentrated virus were resuspended in virus standard buffer (10 mM Tris-hydrochloride, pH 7.4, 10 mM KCl, 5 mM EDTA) with a Dounce homogenizer. The virus suspension was then centrifuged for 40 min at 20,000 rpm at 4°C on a sucrose gradient (17 to 30% [wt/vol]) in an SW27 rotor (Beckman Instruments, Inc., Fullerton, Calif.). The opalescent virus band was collected by puncturing the side of the tube and was pelleted by additional centrifugation for 60 min at 20,000 rpm at 4°C in an SW27 rotor. The pellet was resuspended in virus standard buffer and lysed with 2% (wt/vol) Sarkosyl. It was then treated with 100 μg of proteinase K per ml at 60°C for 1 h. The lysate was diluted to 10 ml, adjusted to final concentrations of 10 mM Tris-hydrochloride (pH 7.4), 1 mM EDTA, and 1.715 g of CsCl per ml, and centrifuged at 40,000 rpm at 23°C for 40 h in a 50 Ti rotor (Beckman). The fraction at a density of 1.718 g/cm^3 that contained viral DNA, as revealed by a peak of radioactivity, was collected and dialyzed against 10 mM Tris-hydrochloride (pH 7.4)–1 mM EDTA. The DNA of P3HR-1 EBV-infected BJAB cells was obtained after phenol extraction, as described previously (31).

Cleavage of DNA with restriction endonucleases and gel electrophoresis. The restriction enzymes *Hin*dIII and *Bam*HI were purchased from Bethesda Research Laboratories, Gaithersburg, Md., or Boehringer, Mannheim, Federal Republic of Germany. DNA was digested with 5 U of enzyme per μg of DNA at 37°C for 3 h. After ethanol precipitation, samples were loaded onto 0.4% (*Hin*dIII digests) or 0.7% (*Bam*HI digests) horizontal agarose gels. Electrophoresis was carried out at 40 V for 15 h.

Preparation of recombinant plasmids. The recombinant pACYC 184 plasmids described in this paper were obtained by subcloning cosmid clones containing the *Sal*I and *Hin*dIII fragments of M-ABA EBV DNA. The overlapping cosmid clones of M-ABA EBV DNA and the subclones derived from such cosmid clones have been described in detail elsewhere (2; A. Polack, G. Hartl, U. Zimber, U.-K. Freese, G. Laux, K. Takaki, B. Hohn, L. Gissmann, and G. W. Bornkamm, submitted for publication). In some cases, *Bam*HI fragments were directly prepared from the clones by using absorbent malachite green as described by Koller et al. (16).

Radioactive labeling of DNA. [^{32}P]DNA fragment probes were made by nick translation (23) of 0.2 to 1 μg of individual cloned EBV DNA fragments or noncloned *Bam*HI DNA fragments. The cloned EBV DNA fragments were not separated from the vector pACYC184. A ^{32}P-labeled probe representing the EBV genome was made by nick translation pf P3HR-1 virus DNA.

Blot hybridization. DNA fragments were transferred to nitrocellulose filters (Schleicher and Schüll, Dassel, Federal Republic of Germany) as described by Southern (25) with the modifications of Wahl et al. (26). The nitrocellulose filters were then preincubated at least 5 h (usually overnight) at 42°C in a solution containing 50% formamide, 5× SSC (1× SSC is 0.15 M sodium chloride plus 0.015 M sodium citrate), 0.1% bovine serum albumin, 0.1% polyvinylpyrrolidone, 0.1% Ficoll (6), 300 μg of calf thymus DNA per ml, and 50 mM sodium phosphate (pH 6.5). For hybridization, the solution contained 50% formamide, 5× SSC, 0.1% bovine serum albumin, 0.1% polyvinylpyrrolidone, 0.1% Ficoll, 20 mM sodium phosphate (pH 6.5), 100 μg of calf thymus DNA per ml, and the labeled single-stranded probe. Hybridization was performed at 42°C for 3 days. After hybridization, the nitrocellulose strips were washed five times in 0.1× SSC–0.1% sodium dodecyl sulfate at 45°C by constant shaking for 3 h. The filters were dried and exposed to X-ray film (Kodak Royal X-Omat) by using an intensifying screen (Du Pont Cronex Lightning Plus).

RESULTS

***Hin*dIII fragment pattern of the defective P3HR-1 EBV DNA genome.** A nitrocellulose filter containing separated *Hin*dIII fragments of DNA from P3HR-1 virus-infected BJAB cells and, for comparison, *Hin*dIII fragments of DNA isolated from P3HR-1 virus particles was hybridized with ^{32}P-labeled P3HR-1 EBV DNA. Autoradiography revealed six hypermolar fragments in DNA from P3HR-1 virus-infected BJAB cells (Fig. 1A, lane a). These six fragments are present in abundant amounts and are much more prominent than the other viral fragments which make up the complete viral genome and which are present in molar amounts. These latter "regular" fragments, for which physical maps have been constructed (1), are not visible in the DNA of P3HR-1-infected BJAB cells (Fig. 1A, lane a) but can be observed after long-term exposure. Four of the six hypermolar fragments, A′, C′, E″, and E‴, do not comigrate with fragments of the nondefective genome and were designated according to their molecular weights in comparison to the fragments of the nondefective genome. Thus for example, E′, E″, E‴, and E⁗ are fragments migrating between *Hin*dIII fragments E and F. Fragments D1 and K2 comigrate with the *Hin*dIII fragments D1 and K2. As will be shown below, *Hin*dIII-K2 and probably also *Hin*dIII-D1 are identical with K2 and D1, respectively, of the nondefective genome. The six fragments were also observed in the *Hin*dIII fragment pattern of P3HR-1 EBV DNA but not in such abundance. Since the fragments of the defective and nondefective genomes can both be visualized by a labeled probe of M-ABA virus DNA which does not contain defective genomes (1), it is obvious that the hypermolar fragments of the defective genome must contain sequences that are also present in fragments of the nondefective genome but differently arranged or bound to cellular sequences.

Hybridization of cloned M-ABA EBV DNA fragments to *Hin*dIII fragments of the defective genome. To elucidate the arrangement of viral sequences in the defective genomes, nitrocellulose filters containing separated *Hin*dIII fragments of DNA from P3HR-1 virus-infected BJAB cells and from

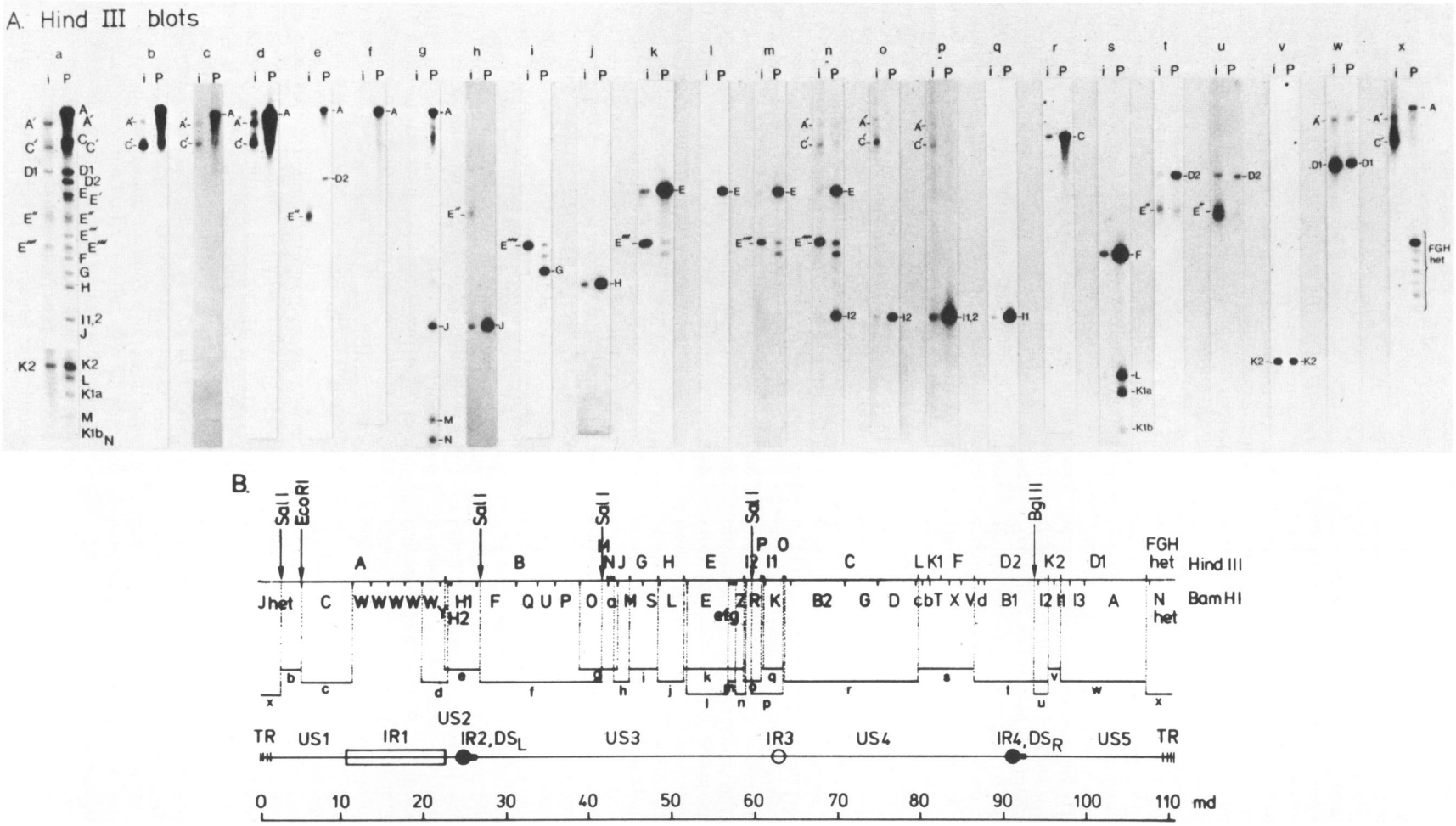

FIG. 1. (A) Hybridization of ^{32}P-labeled P3HR-1 virus DNA (lane a) or ^{32}P-labeled viral DNA fragments (lanes b through x) to nitrocellulose filters containing separated *Hin*dIII fragments of DNA of P3HR-1 virus-infected BJAB cells (i) or of P3HR-1 virus DNA (P). The lower part of lane a was deliberately overexposed to visualize the small fragments (*Hin*dIII fragments K2 through N). The designations of fragments of the defective and nondefective P3HR-1 virus genomes are shown to the left and right of lane a. The location of probes used in (A) on the M-ABA virus map is shown in (B). Probes l, m, and n were isolated from clones containing larger inserts by preparative electrophoresis onto malachite green coupled to polyacrylamide. All other probes were cloned M-ABA virus DNA fragments. The general structure of the EBV genome is adopted from Cheung and Kieff (3) and is shown in the lower part of (B). TR and IR designate terminal and internal repeats, respectively, and U_{S1} through U_{S5} designate the different regions of the viral genome separated from each other by clusters of repeats.

P3HR-1 virus particles were hybridized to a set of cloned M-ABA virus probes representing the complete viral genome of an EBV prototype strain. In some instances, fragments generated by digestion of cloned DNA with *Bam*HI were isolated from the gel, labeled by nick translation, and used as probes. The location of the probes on the viral genome and the results of the hybridization are shown in Fig. 1. *Hin*dIII fragment C′ of the defective genome hybridized to the terminal fragment (Fig. 1A, lane x) and the adjacent fragments of the short unique region, including the large internal repeat (lanes b, c, and d). Additionally it hybridized to sequences located in *Hin*dIII-I2 and *Bam*HI-Z in the right part of the third unique region U_{S3} (lanes n and o). *Hin*dIII-D1 of the defective genome hybridized to M-ABA EBV *Hin*dIII-D1 (lane w).

Fragment A′ hybridized to all of the probes of M-ABA (EBV) DNA which also hybridized to *Hin*dIII-C′ and *Hin*dIII-D1. The size of *Hin*dIII-A′ is 25 megadaltons (Md) and represents a fusion fragment between *Hin*dIII-C′ (15 Md) and *Hin*dIII-D1 (10 Md). Since this fragment is not cleaved by *Hin*dIII, it is obvious that it does not contain the *Hin*dIII site at the right-hand side of *Hin*dIII-D1. *Hin*dIII-D1 of the defective DNA did not hybridize to DNA of the clone containing the terminal *Hin*dIII-*Sal*I fragment (Fig. 1A, lane x), thus excluding the possibility that it is a fusion fragment carrying terminal repeats. *Hin*dIII-E″ of the defective genome hybridized to cloned DNA containing the right-hand side of M-ABA (EBV) *Sal*I-A (lane e), to *Hin*dIII-J (lane h), and to *Hin*dIII-D2 (lane t). The probes used in lanes e and t carry the cross-hybridizing regions DS_L and DS_R (14, 21), so that it cannot be decided whether *Hin*dIII-E″ contains sequences from DS_L or DS_R or from both fragments. Making the assumption that *Hin*dIII-E″ would contain neighboring sequences of the region, from which the cross-hybridizing sequences would be derived, *Hin*dIII-E″ was hybridized to DNA of a clone containing the right-hand part of *Hin*dIII-D2 with the DS_R region excluded (lane u). The positive hybridization to this clone indicated that the sequences in *Hin*dIII-E″ are indeed derived from DS_R. *Hin*dIII-E′′′′ hybridized to cloned M-ABA virus probes *Hin*dIII-G (lane i) and *Hin*dIII-E (lane k) and to the small *Bam*HI fragment located between *Bam*HI-E and *Bam*HI-Z (lane m). *Hin*dIII-K2 of the defective genome hybridized only to the M-ABA (EBV) *Hin*dIII-K2 probe, indicating that this fragment is identical in the defective and nondefective genomes and does not contain rearranged viral sequences. Because of its presence in the defective as well as the nondefective genome, this fragment may be slightly more abundant than fragments only observed in the defective molecules.

Defective genome composed of four nonadjacent regions of the viral genome. The analysis of the experiment shown in Fig. 1 indicated that four nonadjacent regions of the nondefective genome contribute to the formation of the defective DNA population. In order of size, these regions are here designated α, β, γ, and δ. The largest region, α, is located at the right-hand side of the nondefective genome and contains sequences of *Hin*dIII-D2, *Hin*dIII-K2, and *Hin*dIII-D1. The corresponding fragments of the defective genomes with sequences from α are *Hin*dIII-D1, *Hin*dIII-K2, *Hin*dIII-E″, and *Hin*dIII-A′.

The second region of the nondefective genome contributing to the formation of defectives is β, and it contains sequences from the terminus, the complete short unique region (U_{S1}), and sequences from the large internal 3.1-kilobase repeat. The fragments of the defective genomes containing sequences from β are *Hin*dIII-A′ and *Hin*dIII-C′.

The third region, γ, contains sequences of *Hin*dIII-J and *Hin*dIII-G. The fragments of the defective genomes containing sequences from this region are *Hin*dIII-E″ and *Hin*dIII-E′′′′.

The fourth region, δ, is also located in the middle of the nondefective genome and carries sequences from *Hin*dIII-E and *Hin*dIII-I2. The sequences from δ are found in the fragments *Hin*dIII-A′, *Hin*dIII-C′, and *Hin*dIII-E′′′′ of the defective DNA population (for a summary, see Fig. 3A and B).

The arrangement of the four regions α, β, γ, and δ in the defective population could also be deduced from the hybridization data shown in Fig. 1. Thus, the left-hand side of the α region must be joined to the left-hand side of δ, since the *Hin*dIII E″ fragment contains sequences of *Hin*dIII-D2 and *Hin*dIII-J. The right-hand side of the γ region must be adjacent to the left-hand side of δ, since sequences from *Hin*dIII-G and *Hin*dIII-E are found in the same *Hin*dIII E′′′′ fragment. The other side of the δ region must be joined to the β region, since sequences from *Hin*dIII-A and *Hin*dIII-I2 are found in the same *Hin*dIII C′ fragment. The analysis of the breakpoints between the four nonadjacent regions indicates that in the defective population the γ and δ regions have the opposite orientation relative to the α and β regions compared with their orientation in the nondefective genome.

Fine mapping of the sites of recombination in the defective genomes. To characterize in more detail the sites of recombination, a map of the *Bam*HI sites in the defective molecules was constructed. This was done by hybridization of nitrocellulose filters containing separated *Bam*HI fragments of DNA from P3HR-1 virus-infected BJAB cells and from P3HR-1 virus particles with a set of cloned M-ABA virus DNA probes containing sequences of the four regions α, β, γ, and δ, which participate in the formation of the defective molecules. The largest *Bam*HI fragment, BG′, of the defective genome hybridized to cloned DNA containing the left-hand part of the first unique region (U_{S1}) (Fig. 2A, lane b) to *Hin*dIII-D1 (lane r), and to the terminal fragment (lane s). *Bam*HI-BG′ thus consists of sequences different from those of *Bam*HI-BG, which is composed of *Bam*HI-B and *Bam*HI-G and has a molecular mass of ca. 10 Md. *Bam*HI-A hybridized to *Hin*dIII-D1 (lane r) and faintly to the terminal *Hin*dIII-*Sal*I fragment (lane s). The ladder-like pattern of fragments hybridizing to probes containing the left-hand part of the first unique region (U_{S1}) (lane b) and to the terminal fragment (lane s) was not identical to that of the terminal fragments *Bam*HI (J + N)het of nondefective virus DNA. It was therefore designated *Bam*HI Jhet′. *Bam*HI BG′ hybridized to all of the probes of M-ABA EBV DNA which hybridized to *Bam*HI-A and *Bam*HI-Jhet′. We thus concluded that *Bam*HI-A is fused to *Bam*HI-Jhet′, giving rise to *Bam*HI-BG′ in a way similar to that described for *Hin*dIII-A′. As discussed above, the point of the fusion in *Bam*HI-A must be located to the left of the *Bam*HI and *Hin*dIII sites at the right-hand side of *Bam*HI-A. The hybridization to *Bam*HI fragments C (lane c), X1l1 (lanes m, p, q, and r), W (lanes c, d, and e), Z (lanes j and k), and e (lane i) indicated that these fragments are identical in the defective and nondefective genomes and do not contain rearranged viral sequences. *Bam*HI-C′ hybridized to the probes containing *Bam*HI-M (lane f), *Hin*dIII-J (lane g), and *Hin*dIII-D2 (lane m) and to two *Bgl*II fragments which contain DS_R and the right-hand part of *Hin*dIII-D2 without the DS_R region (lanes o and p). Thus *Bam*HI-C′ is a fragment obtained by fusion between the left-hand part of the γ region and the left-hand part of the α region (see Fig. 3C). *Bam*HI-

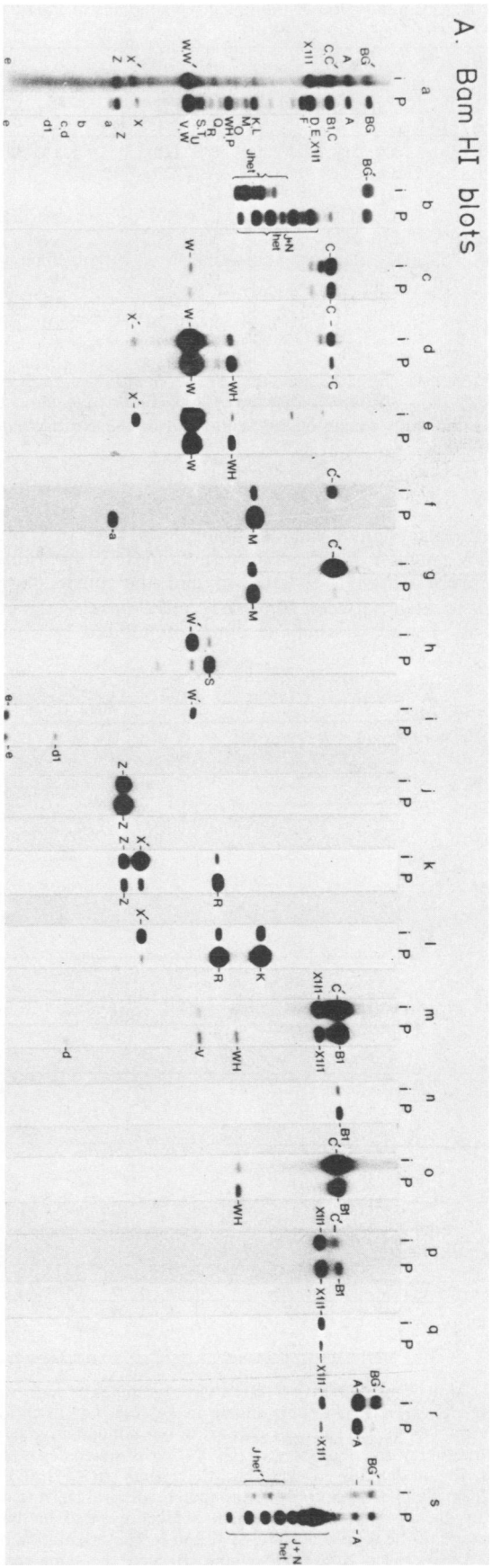

FIG. 2. (A) Hybridization of ^{32}P-labeled P3HR-1 virus DNA (lane a) or ^{32}P-labeled viral DNA fragments (lanes b through s) to nitrocellulose filters containing separated *Bam*HI fragments of DNA of P3HR-1 virus-infected BJAB cells (i) or of P3HR-1 virus DNA (P). The designations of fragments of the defective and nondefective genomes are shown on the left and right of lane a. The location of the probes used in (A) on the M-ABA virus map is shown in (B). Probes f, g, i, and j were isolated from clones containing larger inserts by electrophoresis onto malachite green coupled to polyacrylamide. All other probes were cloned M-ABA virus DNA fragments. TR and IR designate terminal and internal repeats, respectively, and U_{S1} through U_{S5} designate the different regions of the viral genome separated from each other by clusters of repeats.

TABLE 1. Composition of the defective genomes of P3HR-1 virus[a]

Defective *Hin*dIII fragments (Md)	Regular *Hin*dIII fragments	Defective *Bam*HI fragments (Md)	Regular *Bam*HI fragments
A′ (24.8)	ΔA, ΔI_2, ΔD1	BG′ (10)	ΔA, ΔJhet
C′ (14.6)	ΔA, ΔI_2	A (7.7)	A
D1 (10.2)	D1	C (6.2)	C
E″ (≈6)	ΔJ, ΔD_2	C′ (≈6)	ΔM, ΔB1
E″″ (4.3)	ΔE, ΔG	X1I1 (5.3)	X1I1
K_2 (1.3)	K_2	Jhet′	ΔJhet
		W (2.0)	W
		W′ (1.95)	ΔS, Δd1
		X′ (1.30)	ΔW, ΔR
		Z (1.15)	Z
		e (0.31)	e

[a] A′ is C′ plus ΔD1. BG′ is ΔA plus Jhet′, two W fragments. The symbol Δ indicates a part of the sequences of the corresponding fragment.

C′ (6 Md) is slightly smaller than *Bam*HI-C (6.2 Md). *Bam*HI-W′, which comigrated with *Bam*HI-W, hybridized to the probes *Bam*HI-S (lane h) and the small *Bam*HI fragment located between *Bam*HI-E and *Bam*HI-Z (lane i). *Bam*HI-W′ is thus a small fragment generated by fusion between the right-hand part of the γ region and the left-hand part of the δ region. *Bam*HI-W′ has a molecular mass of ca. 1.9 Md and is located in *Hin*dIII-E″″ (see Fig. 3C). *Bam*HI-X′ hybridized to the probes containing *Bam*HI-W (lane d), *Bam*HI-Y, which contains sequences of *Bam*HI-W (lane e), and *Hin*dIII-I2 (lane k). It is thus concluded that *Bam*HI-X′ is a fragment obtained by fusion between the right-hand part of the β region and the right-hand part of the δ region. *Bam*HI-X′ is a small fragment with a molecular mass of ca. 1.3 Md and is located in *Hin*dIII-C′.

Concatemer formation. From the analysis of the breakpoints described above and the sizes of the *Hin*dIII and *Bam*HI fragments in the defective DNA population (Table 1), the map of *Bam*HI and *Hin*dIII sites was established in one repeat unit of the defective molecules (Fig. 3C). From the compilation of the sizes of the *Hin*dIII fragments C′, D1, E″, E″″, and K2, the size of one defective genome unit was calculated to be ca. 36 Md. The sizes of the four nonadjacent regions α, β, γ, and δ, which participate in the formation of the defective genomes, could not be evaluated exactly, since the sites of recombination are not yet precisely determined within the *Bam*HI fusion fragments X′, W′, C′, and BG′. The approximate sizes of the α, β, γ, and δ regions are 17 Md, <13.2 Md, <3.7 Md, and 3 Md, respectively. Two defective genome units can be fused together in tandem configuration, since *Hin*dIII-A′ and *Bam*HI-BG′ represent fusion fragments of the α and β regions. The exact position

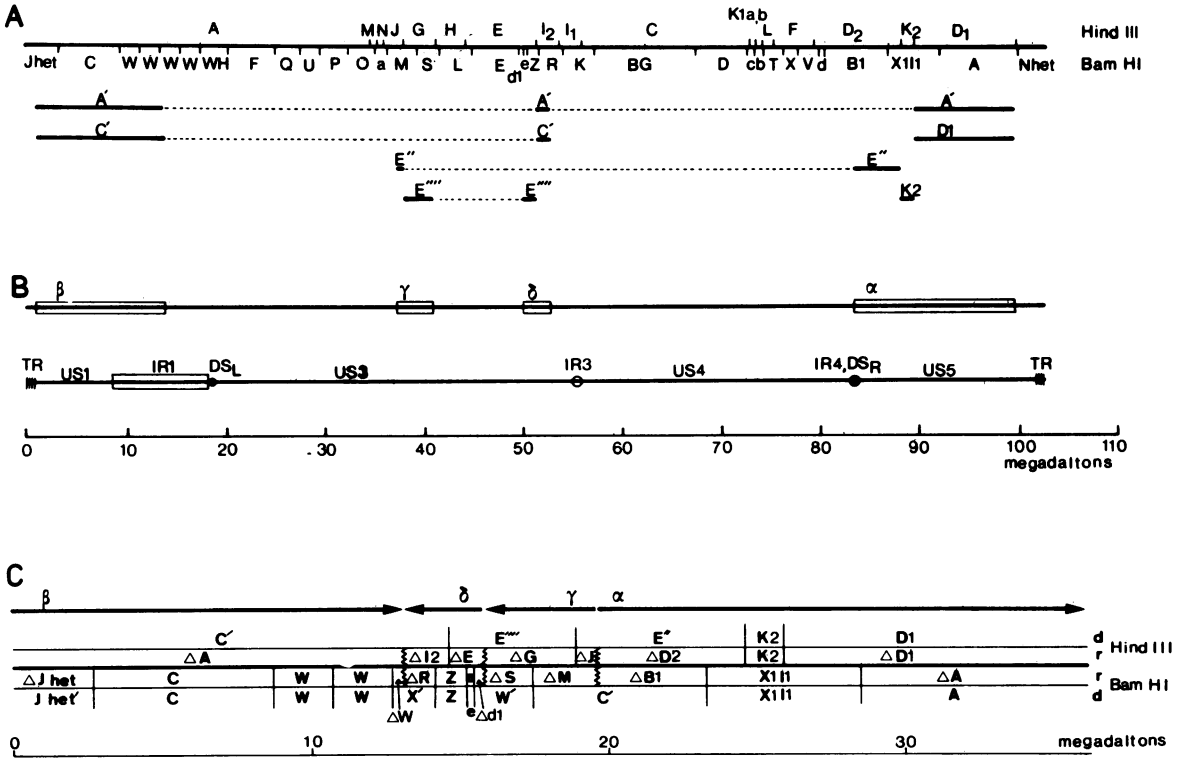

FIG. 3. Map of the defective P3HR-1 virus genomes as suggested by the hybridization data shown in Fig. 1 and 2 and the molecular masses of *Hin*dIII and *Bam*HI fragments shown in Table 1. (A) Location of the *Hin*dIII fragments of the defective genomes on the nondefective P3HR-1 virus DNA. (B) The four regions of the nondefective genome generating the defective genomes are designated α, β, γ, and δ. The general structure of the nondefective P3HR-1 virus molecules is shown below. In P3HR-1 virus DNA the large internal repeats (IR1) are fused to the DS_L region deleting U_{S2} and the DS_L repeats (IR2) (2). (C) Map of the *Hin*dIII and *Bam*HI fragments of the defective genomes (d) that explains from which fragments of the nondefective viral DNA (r) these fragments are derived. The symbol Δ indicates that only part of the sequences of the corresponding fragment are represented in the fragment of the defective genome. The zigzag lines mark the sites of recombination of the four regions α, β, γ, and δ. The orientation of α, β, γ, and δ with respect to their orientation in the nondefective genome is indicated by arrows. Note that (A) and (B) have the same scale, which is different from that of (C).

of the fusion point is not known. To generate *Hin*dIII-A′ and *Bam*HI-BG′, the joint apparently has to be located within *Hin*dIII-D1 and *Bam*HI-A. This is, however, not true for the whole population of molecules. The situation is additionally complicated by the fact that the sequences of *Hin*dIII-D1 and *Bam*HI-A are not exclusively found in the fusion fragments *Hin*dIII-A′ and *Bam*HI-BG′, but also in fragments with the electrophoretic mobility of *Hin*dIII-D1 and *Bam*HI-A. One possible explanation is that these fragments of the defective genomes are not identical to those of the nondefective genomes and represent terminal fragments in linear defective molecules. The absence of terminal repeats in these fragments of the defective population (Fig. 1A, lane x; Fig. 2A, lane s), however, strongly argues against this possibility.

Alternatively, the fusion points between different repeat units of the defective genomes might be heterogeneous and might be located either close to the left or close to the right of the *Hin*dIII and *Bam*HI sites at the right-hand side of *Hin*dIII-D1 and *Bam*HI-A, respectively. The faint hybridization of *Bam*HI-A to the slightly overlapping terminal *Hin*dIII-*Sal*I fragment (Fig. 2A, lane s) argues for this possibility. Thus, it seems likely that not only *Hin*dIII-A′ and *Bam*HI-BG′ but also *Hin*dIII-C′ and *Bam*HI-Jhet′ represent fusion fragments between the α and β regions (Fig. 4). The inability to identify a fragment in the defective DNA population, which might represent the right-hand terminus in linear molecules (Fig. 1A, lane x; Fig. 2A, lane s), additionally suggests that during replication in BJAB cells large concatemers or circles of defective viral DNA are formed.

DISCUSSION

We studied the structural organization of defective P3HR-1 EBV DNA after infection of the EBV-negative BJAB cells with P3HR-1 virus.

Earlier studies concerned with the structure of the defective DNA have always been done with P3HR-1 virus preparations which consist of a mixture of defective and nondefective viral genomes in which the nondefective population is dominant (1, 5, 10). The representation of certain regions of the wild-type genome in the defective population of P3HR-1 virus has been reported by Heller et al. (10) with comparable but not identical results to those described here. The interpretation of their data, however, was hampered by the fact that these authors also studied a mixed population of nondefective and defective molecules, so that it was impossible to establish a restriction enzyme linkage map of the defective genomes.

The use of P3HR-1 virus-infected BJAB cells has been the major breakthrough in our effort to study the structural organization of the defective DNA population. After infection the defective genomes of P3HR-1 virus are preferentially replicated (4). Since BJAB cells do not harbor endogenous EBV genomes, the analysis of the replicating viral DNA molecules is thus largely facilitated.

The results presented here show that the defective P3HR-1 EBV DNA is formed by four distinct regions of the viral DNA, with two large parts (α, 17 Md; β, 13 Md) which flank two small internal parts (γ, 3.7 Md; δ, 3 Md). The two internal regions are inverted compared with their orientation in the nondefective genome. The α and β regions are fused to each other, giving rise to the formation of concatemers or circles.

The structure of the defective genomes shown in Fig. 3 and 4, including the junction points between the α, β, γ, and δ regions, has recently been fully confirmed by the analysis of cloned fragments of the defective genomes (M.-S. Cho, L. Gissmann, and S. D. Hayward, submitted for publication).

The right-hand end of the α region, including the fusion point to β, appeared to be heterogeneous. In some of the molecules it is located to the left of the *Hin*dIII site at the

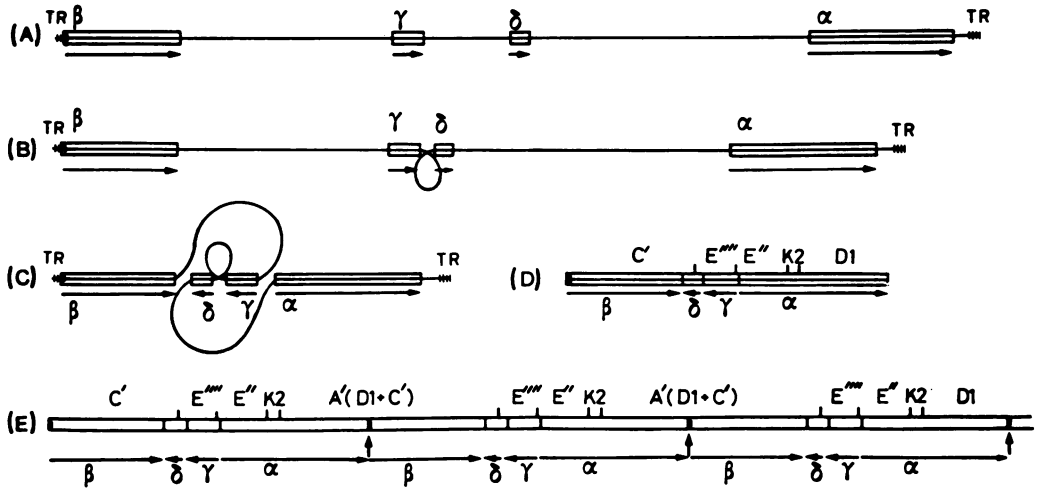

FIG. 4. Model for the generation of defective molecules from the nondefective P3HR-1 virus genome. The location of the four regions which participate in the formation of defective molecules on the nondefective P3HR-1 genome is shown in (A). Intramolecular recombination leads to the fusion of γ and δ (B). The fusion of γ and δ to the regions α and β in opposite orientation compared with the nondefective P3HR-1 genome is shown in (C), leading to the formation of one structural unit of the defective molecules (D). The α and β regions are fused to generate concatemers (E). The fusion sites are indicated by arrows. Terminal repeats (TR) are located very close to the fusion sites. Note that the fusion points between the α and β regions are heterogeneous (E). The letters in (D) and (E) designate the *Hin*dIII fragments of the defective molecules. The intracellularly replicating defective molecules probably form large concatemers or circles. In P3HR-1 cells, linear defective molecules consisting of three structural units can be encapsidated into virions, presumably by using the terminal repeats as packaging signals.

right-hand side of *Hin*dIII-D1, thus giving rise to the fusion fragment *Hin*dIII-A′, which is not cut by *Hin*dIII. This fragment corresponds to *Bam*HI-BG′. In some of the molecules, however, the fusion point appeared to be to the right of the *Hin*dIII site and the neighboring *Bam*HI site. In these molecules *Hin*dIII-D1 and *Bam*HI-A are completely conserved. According to this model *Hin*dIII-C′ and *Bam*HI-Jhet′ also represent fusion fragments in the second population of defective genomes.

Whether the population of defective genomes is intracellularly present in circular form or as large linear concatemers cannot be decided from the data presented. Our inability to detect two distinct terminal fragments argues against the possibility that concatemers of only a few defective genome units are present in linear form in the population replicating in BJAB cells. This is in contrast to the observations made by studying the defective genomes in P3HR-1 virus preparations. Starting from virion DNA, both termini of the defective population can readily be detected (1, 10).

The simplest hypothesis is to assume that upon viral DNA replication in P3HR-1 cells, concatemers consisting of three or four defective genome units are linearized at the terminal repeats and become encapsidated into virus particles. This is in agreement with our earlier partial denaturation studies, which suggested that the most common nonstandard P3HR-1 virus DNA consists of repeat units of 30 to 40 Md (5). These linearized molecules, however, are only formed during packaging, but it is not clear whether the intracellularly replicating defective genomes in P3HR-1-infected BJAB cells are linear or circular.

When the partial denaturation patterns of the four nonadjacent regions in the nondefective molecules are reconstructed as rearranged defective molecules, this reconstructed pattern is virtually identical with the one of each repeat unit described in the denaturation pattern of the defective population (data not shown). Thus, the map of the defective molecules described in this paper is fully compatible with the results from our previous partial denaturation studies, which provided direct evidence for concatemer formation and for a limited heterogeneity in the population of defective molecules.

The accumulation of defective DNA in the P3HR-1 line may account for the specific biological properties of P3HR-1 EBV in comparison with other EBV isolates. This is also strongly suggested by the work of Heston et al. (12) and Rabson et al. (22). Using single-cell subclones of the P3HR-1 line which either carry or lack defective genomes, these authors were able to link high spontaneous virus production and early antigen-inducing activity of P3HR-1 virus with the presence of defective genomes (22). Moreover, two distinct regions of the wild-type genome which have been shown to be involved in the induction of a nuclear and a cytoplasmic antigen of the early antigen complex (K. Takaki, A. Polack, and G. W. Bornkamm, submitted for publication) are also partially or totally represented in the defective genomes (Cho et al., submitted for publication).

It is now of particular interest to study the biological function of fragments cloned from the defective population in DNA transfer experiments (Cho et al., submitted for publication).

ACKNOWLEDGMENTS

The technical assistance of Pia Reiser is gratefully acknowledged.

This work is supported by the Deutsche Forschungsgemeinschaft (SFB 31, Medizinische Virologie: Tumorentstehung und -entwicklung).

LITERATURE CITED

1. **Bornkamm, G. W., H. Delius, U. Zimber, J. Hudewentz, and M. A. Epstein.** 1980. Comparison of Epstein-Barr virus strains of different origin by analysis of the viral DNAs. J. Virol. **35**:603–618.
2. **Bornkamm, G. W., J. Hudewentz, U. K. Freese, and U. Zimber.** 1982. Deletion of the nontransforming Epstein-Barr virus strain P3HR-1 causes fusion of the large internal repeat to the DS_L region. J. Virol. **43**:952–968.
3. **Cheung, A., and E. Kieff.** 1982. Long internal direct repeat in Epstein-Barr virus DNA. J. Virol. **44**:286–294.
4. **Cho, M.-S., K.-O. Fresen, and H. zur Hausen.** 1980. Multiplicity-dependent biological and biochemical properties of Epstein-Barr virus (EBV) rescued from non-producer lines after superinfection with P3HR-1 EBV. Int. J. Cancer **26**:357–363.
5. **Delius, H., and G. W. Bornkamm.** 1978. Heterogeneity of Epstein-Barr virus. III. Comparison of a transforming and a nontransforming virus by partial denaturation mapping of their DNAs. J. Virol. **27**:81–89.
6. **Denhardt, D. T.** 1966. A membrane-filter technique for the detection of complementary DNA. Biochem. Biophys. Res. Commun. **23**:641–646.
7. **Fresen, K.-O., M.-S. Cho, and H. zur Hausen.** 1978. Recovery of transforming EBV from non-producer cells after superinfection with non-transforming P3HR-1 EBV. Int. J. Cancer **22**:378–383.
8. **Fresen, K.-O., B. Merkt, G. W. Bornkamm, and H. zur Hausen.** 1977. Heterogeneity of Epstein-Barr virus originating from P3HR-1 cells. I. Studies on EBNA induction. Int. J. Cancer **19**:317–323.
9. **Fresen, K.-O., and H. zur Hausen.** 1976. Establishment of EBNA-expressing cell lines by infection of Epstein-Barr virus (EBV)-genome-negative human lymphoma cells with different EBV strains. Int. J. Cancer **17**:161–166.
10. **Heller, M., T. Dambaugh, and E. Kieff.** 1981. Epstein-Barr virus DNA. IX. Variation among viral DNAs from producer and nonproducer infected cells. J. Virol. **38**:632–648.
11. **Henle, W., G. Henle, B. A. Zajac, G. Pearson, R. Waubke, and M. Scriba.** 1970. Differential reactivity of human serums with early antigens induced by Epstein-Barr virus. Science **169**:188–190.
12. **Heston, L., M. Rabson, N. Brown, and G. Miller.** 1982. New Epstein-Barr virus variants from cellular subclones of P3HR-1 Burkitt lymphoma. Nature (London) **295**:160–163.
13. **Hinuma, Y., M. Konn, D. J. Yamaguchi, D. J. Wudarski, J. R. Blakeslee, Jr., and J. Y. Grace, Jr.** 1967. Immunofluorescence and herpes-type virus particles in the P3HR-1 Burkitt lymphoma cell line. J. Virol. **1**:1045–1051.
14. **Hudewentz, J., H. Delius, U. K. Freese, U. Zimber, and G. W. Bornkamm.** 1982. Two distant regions of the Epstein-Barr virus genome with sequence homologies have the same orientation and involve small tandem repeats. EMBO J. **1**:21–26.
15. **Klein, G., T. Lindahl, M. Jondal, W. Leibold, J. Menézes, K. Nilsson, and C. Sundström.** 1974. Continuous lymphoid cell lines with characteristics of B cells (bone-marrow-derived), lacking the Epstein-Barr virus genome and derived from three human lymphomas. Proc. Natl. Acad. Sci. U.S.A. **71**:3283–3286.
16. **Koller, B., H. Delius, H. Bunemann, and W. Muller.** 1978. The isolation of DNA from agarose gels by electrophoretic elution onto malachite green-polyacrylamide columns. Gene **4**:227–239.
17. **Lee, Y.-S., Y. Yajima, and M. Nonoyama.** 1977. Mechanism of infection by Epstein-Barr virus. II. Comparison of viral DNA from HR-1 and superinfected Raji by restriction enzymes. Virology **81**:17–24.
18. **Menezes, J., P. Patel, H. Dussault, and A.-E. Bourkas.** 1978. Comparative studies on the induction of virus-associated nuclear antigen and early antigen by lymphocyte-transforming (B95-8) and non-transforming (P3HR-1) strains of Epstein-Barr virus. Intervirology **9**:86–94.
19. **Miller, G., L. Robinson, L. Heston, and M. Lipman.** 1974. Differences between laboratory strains of Epstein-Barr virus

based on immortalization, abortive infection and interference. Proc. Natl. Acad. Sci. U.S.A. **71**:4006–4010.
20. **Pulvertaft, R. J. V.** 1965. A study of malignant tumors in Nigeria by short term tissue culture. J. Clin. Pathol. **18**:261–273.
21. **Raab-Traub, N., T. Dambaugh, and E. Kieff.** 1980. DNA of Epstein-Barr virus. VIII. B95-8, the previous prototype, is an unusual deletion derivative. Cell **22**:257–267.
22. **Rabson, M., L. Heston, and G. Miller.** 1983. Identification of a rare Epstein-Barr virus variant that enhances early antigen expression in Raji cells. Proc. Natl. Acad. Sci. U.S.A. **83**:2762–2766.
23. **Rigby, P. W. J., M. Diekman, C. Rhodes, and P. Berg.** 1977. Labeling deoxyribonucleic acid to high specific activity in vitro by nick translation with DNA polymerase I. J. Mol. Biol. **113**:237–251.
24. **Shaw, J. E., T. Seebeck, H. Li Jui-Lien, and J. S. Pagano.** 1977. Epstein-Barr virus DNA synthesized in superinfected Raji cells. Virology **77**:762–771.
25. **Southern, E. M.** 1975. Detection of specific sequences among DNA fragments separated by gel electrophoresis. J. Mol. Biol. **98**:503–517.
26. **Wahl, G. M., M. Stern, and G. R. Stark.** 1979. Efficient transfer of large DNA fragments from agarose gels to diazobenzyloxymethyl-paper and rapid hybridization by using dextran sulfate. Proc. Natl. Acad. Sci. U.S.A. **76**:3683–3687.
27. **Yajima, Y., B. Marcynska, and M. Nonoyama.** 1978. Transforming activity of Epstein-Barr virus obtained by superinfection of Raji cells. Proc. Natl. Acad. Sci. U.S.A. **75**:2008–2010.
28. **Yajima, Y., and M. Nonoyama.** 1976. Mechanisms of infection with Epstein-Barr virus. I. Viral DNA replication and formation of noninfectious virus particles in superinfected Raji cells. J. Virol. **19**:187–194.
29. **zur Hausen, H., G. W. Bornkamm, R. Schmidt, and E. Hecker.** 1979. Tumor initiators and promoters in the induction of Epstein-Barr virus. Proc. Natl. Acad. Sci. U.S.A. **76**:282–285.
30. **zur Hausen, H., F. J. O'Neill, U. K. Freese, and E. Hecker.** 1978. Persisting oncogenic herpesvirus induced by tumor promoter TPA. Nature (London) **272**:373–375.
31. **zur Hausen, H., H. Schulte-Holthausen, G. Klein, W. Henle, G. Henle, P. Clifford, and L. Santesson.** 1970. EBV-DNA in biopsies of Burkitt tumours and anaplastic carcinomas of the nasopharynx. Nature (London) **228**:1056–1058.